Acta Crystallographica Section C
Crystal Structure Communications
ISSN 0108-2701

Tl_2Te and its relationship with Tl_5Te_3

Radovan Černý,[a]* Jean-Marc Joubert,[b] Yaroslav Filinchuk[a] and Yves Feutelais[c]

[a]Laboratoire de Cristallographie, Université de Genève, 24 quai Ernest-Ansermet, CH-1211 Genève 4, Switzerland, [b]Laboratoire de Chimie Métallurgique des Terres Rares, CNRS, 2-8 rue Henri Dunant, 94320 Thiais, France, and [c]Laboratoire de Chimie Physique, Minérale et Bioinorganique, EA 401, Faculté de Pharmacie, 5 rue J.-B. Clément, 92296 Châtenay-Malabry, France
Correspondence e-mail: radovan.cerny@cryst.unige.ch

Received 26 October 2001
Accepted 19 March 2002
Online 19 April 2002

The crystal structure of Tl_2Te, dithallium telluride, has been determined by single-crystal X-ray diffraction. The analysis of the structure shows that this compound is the first known representative of a new crystal structure type. The structural relationship with the related Tl_5Te_3 phase is discussed.

Comment

Although the existence of Tl_2Te has been reported by many authors (Hahn & Klinger, 1949; Rabenau *et al.*, 1960; Vasilev *et al.*, 1968; Asadov *et al.*, 1977; Chami *et al.*, 1983), its crystal structure has remained undetermined and its existence has even been questioned (Chikashige, 1912; Klemm & Vogel, 1934; Oh & Lee, 1993). Using differential scanning calorimetry and powder X-ray diffraction, a study of the Tl–Te phase diagram was undertaken by Record *et al.* (1997), in which the existence of this phase was unambiguously confirmed. We report here on the crystal structure of Tl_2Te and its relation to Tl_5Te_3.

The crystal structure of Tl_2Te can be described as two alternating types of ($h0h$) layers, similar to those found in the structure of Tl_5Te_3 [Fig. 1 in Schewe *et al.* (1989)]. Layer type *A* is a quasi-planar layer at $x + z = 0, \frac{1}{2}, 1$ and $\frac{3}{2}$. Layer type *B* is a puckered layer (thickness 2.5 Å) at $x + z = \frac{1}{4}, \frac{3}{4}, \frac{5}{4}$ and $\frac{7}{4}$. Layer *A* (Fig. 1) corresponds to the layer found at $z = 0$ and $\frac{1}{2}$ in Tl_5Te_3, while layer *B* (Fig. 1) corresponds to the layer found at $z = \frac{1}{4}$ and $\frac{3}{4}$ in Tl_5Te_3.

Layer *A* is described in Tl_5Te_3 as being formed from a 3^2434 net of Te atoms centred by a 4^4 net of Tl atoms. Bands of width ~18.3 Å containing basic motifs of this net are formed from atoms Tl3, Tl4, Te1, Te3, Te4 and Te5 in the structure of Tl_2Te. These bands are oriented along the *b* axis and are repeated twice in the $[10\overline{1}]$ direction of the cell of Tl_2Te. Neighbouring bands are mutually shifted from the ideal infinite nets found in Tl_5Te_3 by a vector lying in the ($h0h$) plane having a length of ~4.85 Å (Fig. 1). The composition of layer *A* is identical in Tl_2Te (Tl_8Te_{16}) and in Tl_5Te_3 (Tl_4Te_8).

Layer *B* is described in Tl_5Te_3 as being formed from a 48^2 net of Tl atoms centred by a 4^4 net of Te atoms. Bands of width ~14.7 Å containing basic motifs of this net are formed from atoms Tl1, Tl2, Tl5, Tl6, Tl7, Tl8, Tl9, Tl10, Tl11, Te2 and Te6 in the structure of Tl_2Te. The bands are also oriented along the *b* axis and are repeated twice in the $[10\overline{1}]$ direction of the cell of Tl_2Te. Neighbouring bands are again mutually shifted by the same vector as in layer *A*, and are separated by atomic chains containing only Tl atoms. The composition of layer *B* in Tl_2Te is $Tl_{36}Te_6$, compared with $Tl_{16}Te_4$ in Tl_5Te_3. The overall composition changes from Tl_5Te_3 to Tl_2Te.

The shears in layers *A* and *B* occur so that they form (002) shear planes. The stacking of layers *A* and *B* in the structure of Tl_2Te, and the relation between the elementary cells of Tl_2Te and Tl_5Te_3, are given in Fig. 2.

The structure of Tl_5Te_3 has also been described as containing infinite straight Te—Tl—Te chains, with Tl—Te distances of 3.15 Å, and quasi-molecular Tl_2Te groups, with Tl—Te distances of 3.16 Å. These chains propagate along the direction perpendicular to layers *A* and *B*. They can also be identified in the structure of Tl_2Te. However, they are finite (Tl4—Te2—Tl3—Te6—Tl3—Te2—Tl4), because of the shears in the *A* and *B* layers, and distorted (Tl—Te distances between 3.14 and 3.34 Å). The Tl_2Te groups can also be found in the structure of Tl_2Te. However, the Tl—Te distance in the group varies between 3.15 and 3.30 Å.

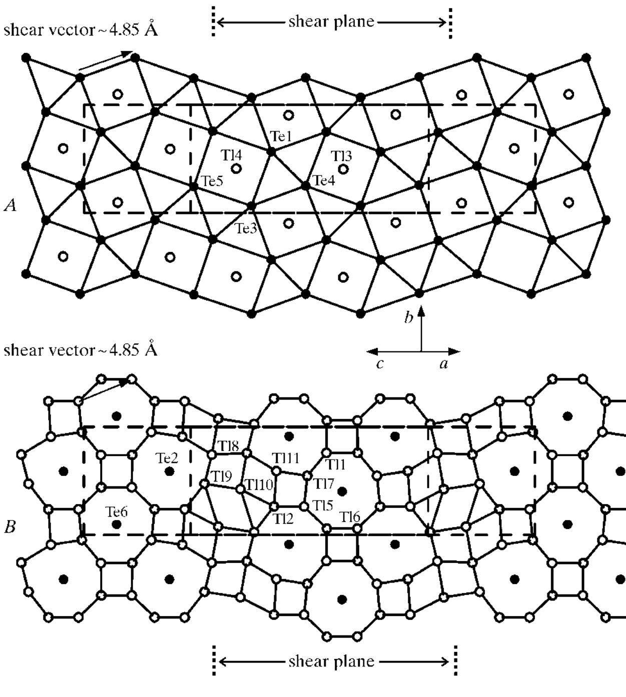

Figure 1
The structure of Tl_2Te viewed in the direction ~[301]. Two basic units, the planar layer *A* and the puckered layer *B*, are shown. Open circles indicate Tl atoms and filled circles indicate Te atoms. Only the Te net in layer *A* and the Tl net in layer *B* are shown. The position of the shear plane is marked by a dashed line in each unit. The shear vector between two Tl_5Te_3-like regions is also shown.

DOI: 10.1107/S0108270102005085

The coordination of Tl and Te atoms in the structure of Tl_2Te is derived from that in the structure of Tl_5Te_3. The Tl atoms lying in the A layer of the Tl_5Te_3 structure are coordinated by a Te_{4+2} octahedron in the first sphere and by a Tl_8 cube in the second sphere. This coordination is nearly preserved in the Tl_2Te structure for atom Tl3, with slightly longer Tl—Te distances (3.30–3.42 Å) in the Te_6 octahedron and in the deformed Tl_8 cube (Tl—Tl distances of 3.82–4.09 Å). For atom Tl4, lying on the shear plane, the coordination is Te_5 (Tl—Te distances of 3.15–3.85 Å) and Tl_8 (Tl—Tl distances of 3.32–3.99 Å).

The Tl atoms in the B layer of the Tl_2Te structure are coordinated in the first sphere in a way similar to the Tl atoms in the B layer of the Tl_5Te_3 structure (distorted trigonal prism, Te_3Tl_3), with Tl—Te distances 3.15–3.54 Å and Tl—Tl distances of 3.35–3.73 Å. The Tl9—Tl4 (3.32 Å), Tl9—Tl8 (3.37 Å) and Tl10—Tl11 (3.35 Å) distances, found near the shear plane, correspond well with the distance in metallic Tl (3.35 Å).

The Te atoms in the A layer of the Tl_2Te structure lying outside the shear plane (atoms Te1, Te3 and Te4) are coordinated in a similar way to the Te atoms in the A layer of the Tl_5Te_3 structure (distorted bicapped trigonal prism, Tl_8), with Te—Tl distances of 3.15–3.58 Å. Atom Te5, lying on the shear plane, is coordinated by a distorted trigonal prism, Tl_6, with Te—Tl distances of 3.30–3.43 Å. Atom Te6, lying in the B layer outside the shear plane, is coordinated as in the Tl_5Te_3 structure, by a compressed bicapped tetragonal antiprism, with Te—Tl distances of 3.31–3.69 Å. Atom Te2, lying in the B layer close to the shear plane, is coordinated by a distorted tetragonal antiprism, with Te—Tl distances of 3.14–3.68 Å.

The crystal structure of Tl_2Te can be rationalized as being composed from regions with the structure of Tl_5Te_3 and regions which contain only Tl atoms, some of them showing Tl—Tl distances corresponding to metallic Tl. This description is further supported by the decomposition of Tl_2Te into Tl_5Te_3 and Tl on heating (Rabenau *et al.*, 1960; Vasilev *et al.*, 1968; Schewe *et al.*, 1989). We have observed such phase transformation on a bulk sample of Tl_2Te, by powder diffraction and Rietveld refinement. After several days of the sample being exposed to air, it had nearly completely transformed to the Tl_5Te_3 phase and thallium oxides. According to the analysis of the Tl_5Te_3 structure by Schewe *et al.* (1989), the bond analysis of the Tl—Te system by Bhan & Schubert (1970), the chemical composition and the absence of Te—Te bonds in the structure of Tl_2Te, we expect that Tl has the oxidation state Tl^{1+} in Tl_2Te, and that the compound is metallic.

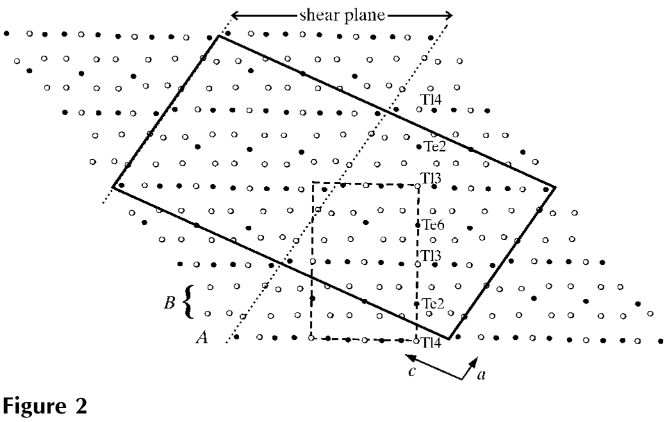

Figure 2
The stacking of layers A and B in the structure of Tl_2Te viewed in the [010] direction. The Tl_2Te cell is shown by a solid line and the Tl_5Te_3 cell by a dashed line. Open circles indicate Tl atoms and filled circles indicate Te atoms. The position of the shear plane is marked by a dashed line.

The structures of Tl_5Te_3 and Tl_2Te are closely related and, indeed, the crystal studied here was intergrown from two domains, one with the Tl_2Te structure and the other having a cubic face-centred lattice, with a_c = 12.70 Å. The diffraction pattern of the Tl_5Te_3 structure shows a strong face-centred cubic pseudosymmetry, with a_c = 12.60 Å, following the relationship $a_t = \frac{1}{2}(-a_c + c_c) = 8.98$ Å, $b_t = \frac{1}{2}(a_c + c_c) = 8.98$ Å and $c_t = b_c = 12.60$ Å. Some authors have even reported a diffraction pattern corresponding to a cubic lattice, with a lattice parameter of approximately 12.60 Å (Man *et al.*, 1971; Anseau, 1973).

The Tl_5Te_3 phase shows a small range of homogeneity of several atomic% Tl. Whether, within this homogeneity range, the structure can change from pseudocubic to true cubic, and whether our second domain corresponds to that cubic structure or to the tetragonal Tl_5Te_3 structure, cannot be answered here, because of the small size of the second domain. The monoclinic cell of the Tl_2Te structure can also be related to the cubic cell with a_c = 12.70 Å. However, the deviation from the cubic lattice is much greater than in the case of the tetragonal Tl_5Te_3 cell. We have observed the following relationship between the lattices of the first domain (monoclinic) and the second domain (cubic) with a_c = 12.70 Å: $a_m \sim \frac{1}{2}(-a_c + 2b_c - c_c) = 15.55$ Å, $b_m = \frac{1}{2}(-a_c + c_c) = 8.98$ Å and $c_m \sim 2a_c + b_c + 2c_c = 28.40$ Å.

Experimental

The analytical sample was composed of weighed samples of pure thallium (Fluka, 4 N, 0.995 g) and pure tellurium (Fluka, 5 N, 0.299 g). Non-soluble impurities were removed from the tellurium by filtration under purified argon on silica wool. The thin oxide layer on the surface of the pure thallium pellets was removed using sulfuric acid baths (0.1 N) followed by rinsing in acetone. The alloy was then formed by direct fusion of the pure elements in a silica tube sealed under vacuum (10^{-1} Pa). The composition of the alloy (x_{Te} = 0.325) was chosen to ensure that the Tl_2Te phase (x_{Te} = 0.333) was obtained even in the event of evaporation or oxidation of the thallium. Subsequent annealing was performed for 160 h at 553 K. For X-ray data collection, the crystal was covered with a protective layer of perfluoropolyalkyl ether (ABCR GmbH & Co.) to prevent its oxidation and decomposition.

Crystal data

Tl_2Te
M_r = 536.37
Monoclinic, $C2/c$
a = 15.6621 (9) Å
b = 8.9873 (4) Å
c = 31.196 (2) Å
β = 100.761 (7)°
V = 4313.9 (4) Å^3
Z = 44

D_x = 9.084 Mg m^{-3}
Mo $K\alpha$ radiation
Cell parameters from 2000 reflections
θ = 3–25°
μ = 89.10 mm^{-1}
T = 293 K
Parallelepiped, metallic dark grey
0.15 × 0.03 × 0.03 mm

Table 1
Selected interatomic distances (Å).

Tl1—Te3	3.266 (3)	Tl5—Te2$^{\text{xi}}$	3.560 (4)
Tl1—Te4	3.356 (4)	Tl5—Tl6	3.592 (3)
Tl1—Te1	3.457 (4)	Tl6—Te4	3.175 (4)
Tl1—Tl7$^{\text{i}}$	3.508 (3)	Tl6—Te4$^{\text{xii}}$	3.453 (4)
Tl1—Tl1$^{\text{ii}}$	3.586 (2)	Tl6—Te1$^{\text{xii}}$	3.462 (3)
Tl1—Tl6$^{\text{iii}}$	3.631 (3)	Tl6—Tl6$^{\text{xiii}}$	3.514 (3)
Tl2—Te4	3.241 (3)	Tl7—Te4$^{\text{viii}}$	3.151 (3)
Tl2—Te3	3.272 (4)	Tl7—Te4	3.297 (4)
Tl2—Te1	3.344 (4)	Tl7—Te6$^{\text{xi}}$	3.396 (3)
Tl2—Tl9$^{\text{iv}}$	3.460 (3)	Tl7—Tl11$^{\text{v}}$	3.421 (2)
Tl2—Tl5	3.514 (3)	Tl8—Te1	3.182 (3)
Tl2—Tl11$^{\text{v}}$	3.692 (3)	Tl8—Te3$^{\text{vii}}$	3.338 (4)
Tl3—Te6	3.3016 (17)	Tl8—Tl9$^{\text{v}}$	3.372 (3)
Tl3—Te2$^{\text{vi}}$	3.329 (3)	Tl8—Te5$^{\text{xiv}}$	3.407 (4)
Tl3—Te1	3.354 (4)	Tl8—Tl11$^{\text{v}}$	3.693 (3)
Tl3—Te3$^{\text{vii}}$	3.403 (3)	Tl8—Tl10$^{\text{vii}}$	3.739 (3)
Tl3—Te4$^{\text{vii}}$	3.417 (4)	Tl9—Te2$^{\text{xiv}}$	3.175 (3)
Tl3—Te4$^{\text{viii}}$	3.422 (3)	Tl9—Te5$^{\text{xiv}}$	3.283 (4)
Tl4—Te2$^{\text{ix}}$	3.154 (3)	Tl9—Te5	3.300 (4)
Tl4—Te1$^{\text{ix}}$	3.234 (4)	Tl10—Te3	3.229 (3)
Tl4—Tl9$^{\text{ix}}$	3.314 (2)	Tl10—Te5	3.293 (4)
Tl4—Te3$^{\text{ix}}$	3.363 (4)	Tl10—Tl11$^{\text{xv}}$	3.335 (3)
Tl4—Te5$^{\text{x}}$	3.676 (4)	Tl10—Te5$^{\text{xvi}}$	3.371 (4)
Tl4—Te5$^{\text{ix}}$	3.846 (4)	Tl11—Te2$^{\text{xiv}}$	3.170 (4)
Tl5—Te1$^{\text{xi}}$	3.186 (4)	Tl11—Te3$^{\text{xiv}}$	3.256 (4)
Tl5—Te3$^{\text{vi}}$	3.397 (4)	Tl11—Te5$^{\text{xiv}}$	3.433 (3)
Tl5—Tl7	3.560 (3)		

Symmetry codes: (i) $\frac{1}{2}+x, \frac{1}{2}+y, z$; (ii) $1-x, y, \frac{3}{2}-z$; (iii) $\frac{1}{2}+x, y-\frac{1}{2}, z$; (iv) $\frac{1}{2}-x, \frac{3}{2}-y, 1-z$; (v) $\frac{1}{2}-x, \frac{1}{2}-y, 1-z$; (vi) $x-\frac{1}{2}, y-\frac{1}{2}, z$; (vii) $x, y-1, z$; (viii) $\frac{1}{2}-x, y-\frac{1}{2}, \frac{3}{2}-z$; (ix) $x, 1-y, z-\frac{1}{2}$; (x) $1-x, y, \frac{1}{2}-z$; (xi) $x-\frac{1}{2}, \frac{1}{2}+y, z$; (xii) $\frac{1}{2}-x, \frac{1}{2}+y, \frac{3}{2}-z$; (xiii) $-x, y, \frac{3}{2}-z$; (xiv) $1-x, 1-y, 1-z$; (xv) $x, 1+y, z$; (xvi) $1-x, 2-y, 1-z$.

Data collection

Stoe IPDS diffractometer
φ oscillation scans
Absorption correction: analytical (*X-RED*; Stoe & Cie, 1999)
$T_{\min} = 0.019$, $T_{\max} = 0.127$
12 622 measured reflections
3865 independent reflections
1989 reflections with $F^2 > 2\sigma(F^2)$

$R_{\text{int}} = 0.153$
$\theta_{\max} = 25.9°$
$h = -19 \rightarrow 19$
$k = -11 \rightarrow 10$
$l = -38 \rightarrow 38$
200 standard reflections
frequency: 10 min
intensity decay: none

Refinement

Refinement on F^2
$R(F) = 0.107$
$wR(F^2) = 0.180$
$S = 2.37$
1982 reflections
150 parameters
Weighting scheme based on measured s.u.'s

$(\Delta/\sigma)_{\max} = 0.001$
$\Delta\rho_{\max} = 8.97$ e Å^{-3}
$\Delta\rho_{\min} = -8.32$ e Å^{-3}
Extinction correction: B–C type 1 Gaussian isotropic (Becker & Coppens, 1974)
Extinction coefficient: 0.005

Two non-coherent domains were identified in the crystal. The first domain had the Tl_2Te structure and the second had a cubic face-centred lattice. The reflections of both domains were separated in the process of integrating the images. From 15 502 measured reflections of the first domain, 2880 reflections were rejected because of overlap with reflections of the second domain and mean $F^2/\sigma(F^2) = 4.6$. In the second domain, 7317 reflections were measured and mean $F^2/\sigma(F^2) = 1.9$. The R factors show no systematic deviation of different reflection groups from the mean, whether in dependence on hkl, F_{obs} or $\sin(\theta)/\lambda$. No warnings of twinning were observed. The value of R_{int} and the difference Fourier maps were calculated using 1989 observed reflections. The highest peaks in the difference Fourier map are within 1 Å of the atom sites.

Data collection: *EXPOSE* in *IPDS Software* (Stoe & Cie, 1999); cell refinement: *CELL* in *IPDS Software*; data reduction: *ADDREF* and *SORTRF* in *Xtal*3.7 (Hall *et al.*, 2000), and *TWIN* in *IPDS Software*; program(s) used to solve structure: *SHELXS*97 (Sheldrick, 1997); program(s) used to refine structure: *LSLS* in *Xtal*3.7; molecular graphics: *ATOMS* (Dowty, 1993); software used to prepare material for publication: *BONDLA* and *CIFIO* in *Xtal*3.7.

Supplementary data for this paper are available from the IUCr electronic archives (Reference: BR1351). Services for accessing these data are described at the back of the journal.

References

Anseau, M. R. (1973). *J. Appl. Phys.* **44**, 3357–3359.

Asadov, M. M., Babanly, M. B. & Kuliev, A. A. (1977). *Inorg. Mater.* **13**, 1137–1140.

Becker, P. J. & Coppens, P. (1974). *Acta Cryst.* A**30**, 148–153.

Bhan, S. & Schubert, K. (1970). *J. Less Common Met.* **20**, 229–235.

Chami, R., Tedenac, J.-C., Brun, G. & Maurin, M. (1983). *Mater. Res. Bull.* **18**, 803–808.

Chikashige, M. (1912). *Z. Anorg. Allg. Chem.* **78**, 68–74.

Dowty, E. (1993). *ATOMS*. Version 2.3. Shape Software, 521 Hidden Valley Road, Kingsport, TN 37663, USA.

Hahn, H. & Klinger, W. (1949). *Z. Anorg. Chem.* **260**, 110–119.

Hall, S. R., du Boulay, D. J. & Olthof-Hazekamp, R. (2000). Editors. *Xtal*3.7 *User's Manual.* University of Western Australia, Australia.

Klemm, W. & von Vogel, H. U. (1934). *Z. Anorg. Allg. Chem.* **219**, 56–62.

Man, L. I., Imamov, R. M. & Pinsker, Z. G. (1971). *Sov. Phys. Crystallogr.* **16**, 94–98.

Oh, C. S. & Lee, D. N. (1993). *J. Phase Equilib.* **14**, 197–204.

Rabenau, A., Stegherr, A. & Eckerlin, P. (1960). *Z. Metallkd*, **51**, 295–299.

Record, M.-C., Feutelais, Y. & Lukas, H. L. (1997). *Z. Metallkd*, **88**, 45–54.

Schewe, I., Boettcher, P. & von Schnering, H. G. (1989). *Z. Kristallogr.* **188**, 287–298.

Sheldrick, G. M. (1997). *SHELXS*97. University of Göttingen, Germany.

Stoe & Cie (1999). *X-RED* (Version 1.19) and *IPDS Software* (Version 2.92). Stoe & Cie, Darmstadt, Germany.

Vasilev, V. P., Nikolskaya, A. V., Gerasimov, Ya. I. & Kusnetzov, A. F. (1968). *Inorg. Mater.* **4**, 914–919.